J Electroceram (2006) 17:381–385
DOI 10.1007/s10832-006-9636-3

Crack formation in MLCCs depending on position with and without post-heat treatment

Dong-Wook Kim · Ji-Hun Kang · Sang-Hyun Park · Hyeon-Cheol Kim · Yeon-Gil Jung · Ungyu Paik

Received: 26 June 2005 / Revised: 29 May 2006 / Accepted: 29 June 2006

Abstract The crack formation behavior and mechanical properties, hardness (H), modulus (E), and fracture toughness (K_{IC}), at each plane of $BaTiO_3$ based multilayer ceramic capacitors (MLCCs) have been investigated and estimated using a nanoindentation technique, including effects of the post-heat treatment and the external electrode on the crack formation and mechanical properties. The crack length in each plane, length (x plane) and width (y plane) planes, has been measured for MLCCs with and without the post-heat treatment, as a function of the distance from the internal electrode. H and E values are 11.5–12.0 GPa and 175–190 GPa, respectively, independent of the plane and the post-heat treatment. The crack length in the x plane is smaller than that in the y plane, which is gradually increased as the indentation position is far away from the internal electrode. The external electrode affects the crack formation in regions near to the internal electrode, showing small crack length till 20 μm from the internal electrode. K_{IC} values in the x plane are larger than those in the y plane. The external electrode affects only the K_{IC} values in the x plane within the error range, without effect of the post-heat treatment.

Keywords MLCCs · Post-heat treatment · Nanoindentation · Mechanical properties · Crack · Electrode

D.-W. Kim · J.-H. Kang · S.-H. Park · H.-C. Kim · Y.-G. Jung (✉)
School of Nano and Advanced Materials Engineering, Changwon National University, Changwon, Kyungnam 641-773, Republic of Korea
e-mail: jungyg@changwon.ac.kr

U. Paik
Department of Ceramic Engineering, Hanyang University, 17 Haengdang-dong, Seongdong-gu, Seoul 133-791, Korea

Introduction

Multilayer ceramic capacitors (MLCCs) continue to be one of the most widely used and the most important passive components in the circuitry of the latest consumptive electronic products [1]. Progress in MLCCs fabricating technology has been driven by need to increase capacitance while at the time maintaining product reliability and lowering production costs [2, 3]. For high capacitance in MLCCs, reducing of the active layer thickness is a much more effective strategy for increasing volume efficiency than increasing of the dielectric constant alone. However, these requirements cause problems, such as cracks and residual stresses formed in MLCCs, due to the difference of density and thermal expansion coefficient between inner layer with electrode and cover layer (margins) without electrode [4, 5]. Therefore, the estimation of crack formation behavior and mechanical properties is a topic of considerable scientific and technological interests in MLCCs technology, which is also relevant to the residual stress.

In the present work, the crack formation behavior and mechanical properties, hardness (H), modulus (E), and fracture toughness (K_{IC}) have been investigated and estimated in each plane of MLCCs with and without the post-heat treatment, using a nanoindentation technique. The effects of the external electrode and the post-heat treatment on the crack formation, the residual stress, and mechanical properties have been observed as well.

Experimental procedure

The MLCC samples used in this investigation were commercial products, showing X7R characteristics. The dimensions of MLCCs specimens are $3 \times 2 \times 1.6$ mm with 330 actives including the cover layer (margins) of $\approx 250\,\mu$m,

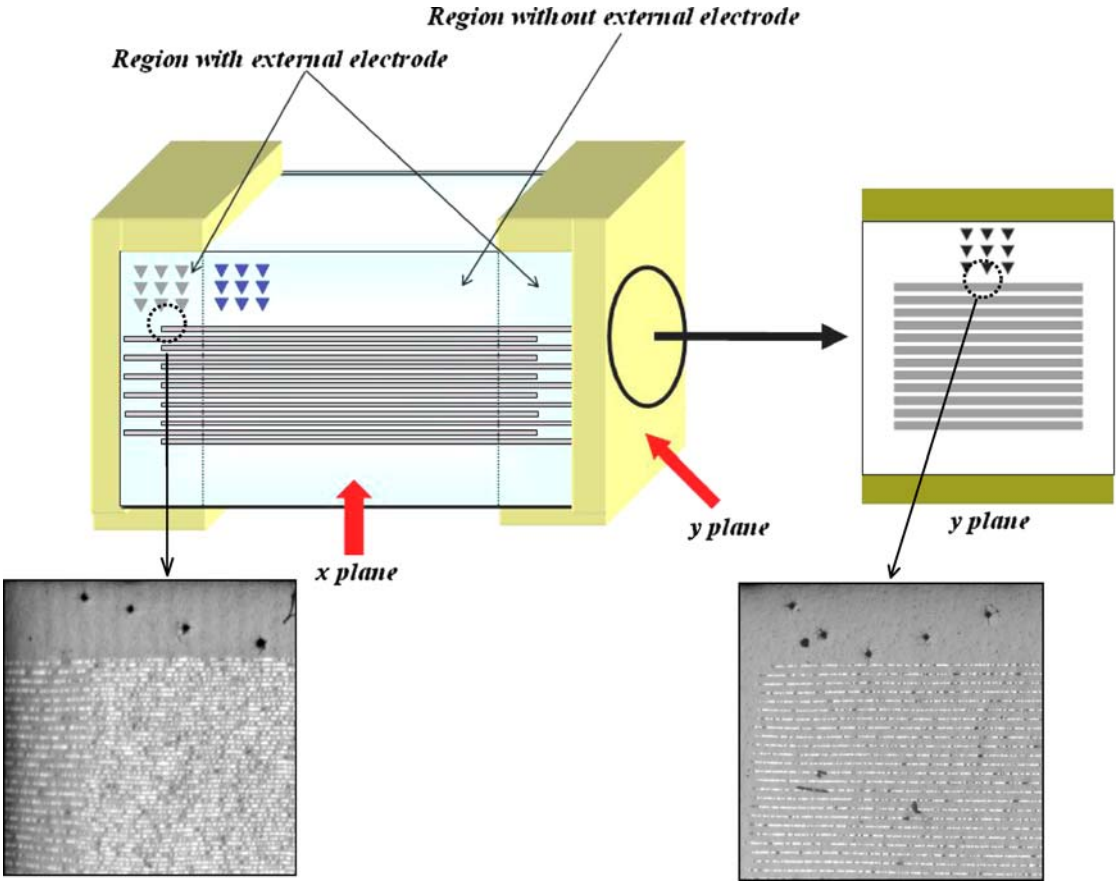

Fig. 1 Schematic diagram of indentation sites in *x* and *y* planes

and the thickness of the dielectric and electrode layers are $\approx 3\,\mu$m and $\approx 2\,\mu$m, respectively. The MLCCs were heat-treated at 900°C with the heating rate of 1°C/min to figure out the effect of the post-heat treatment, which was determined by considering the post-annealing temperature of MLCCs (950°C) after fabrication. Polished samples for an indentation were prepared by initially grinding the MLCCs to a $10\,\mu$m finish, followed by a subsequent final polish to a $1\,\mu$m finish. In addition, to remove residual stress that occurred during the grinding and polishing procedures, the samples were polished with a 10 nm SiO_2 colloid sol.

All indentations were made on the planes of the MLCCs with a nanoindentor (Nano-indenter XP, MTS Systems Corp., Oakridge, TN) using a Berkovich indenter (tip radius <100 nm), considering effects of the external electrode, the distance from the electrode, and the post-heat treatment. The penetration depth was controlled as 750, 1000, and 1250 nm, which are corresponded to the load ranges of 0.1 to 0.3 N. A minimum of five different MLCC samples was indented at each given load. Figure 1 shows a schematic diagram of indentation sites in length (*x* plane) and width (*y* plane) planes for measuring mechanical properties and observing crack formation behavior, including optical micrographs from each cross section. Load-displacement (*P*-*h*) functions are recorded, and hardness and modulus calculated, for each Berkovich nanoindentation [6]. Indentation sites were examined and the crack length was measured with an atomic force microscope (AFM—Digital Instruments Nanoscope IIIa, Veeco Metrology, Santa Barbara, CA) using a gold-coated silicon tip in a contact mode. Also, fracture toughness (K_{IC}) was calculated using the following expression, which has been proposed by Laugier [7]:

$$K_{IC} = 0.0161\left(\frac{a}{l}\right)^{1/2}\left(\frac{E}{H}\right)^{2/3}\frac{P}{c^{3/2}} \tag{1}$$

where c is the crack length measured from the center of contact to end of crack, l is the crack length form the edge of contact to end of crack, a is the half of diagonal indentation, E is the Young's modulus, H is the hardness, and P is the load applied.

Table 1 Hardness and modulus values of MLCCs depending on position and post-heat treatment

Condition property	*X* plane		*Y* plane	
	With	Without	With	Without
	Standard			
Hardness(GPa)	11.64 ± 0.32	11.46 ± 0.25	11.47 ± 0.28	11.06 ± 0.38
Modulus(GPa)	175.5 ± 2.3	181.2 ± 4.5	176.4 ± 5.8	183.2 ± 4.7
	Post-heat treatment(1°C/min to 900°C)			
Hardness(GPa)	12.02 ± 0.38	11.95 ± 0.49	11.75 ± 0.22	11.20 ± 0.64
Modulus(GPa)	183.6 ± 4.7	190.3 ± 3.4	183.9 ± 4.5	182.3 ± 4.1

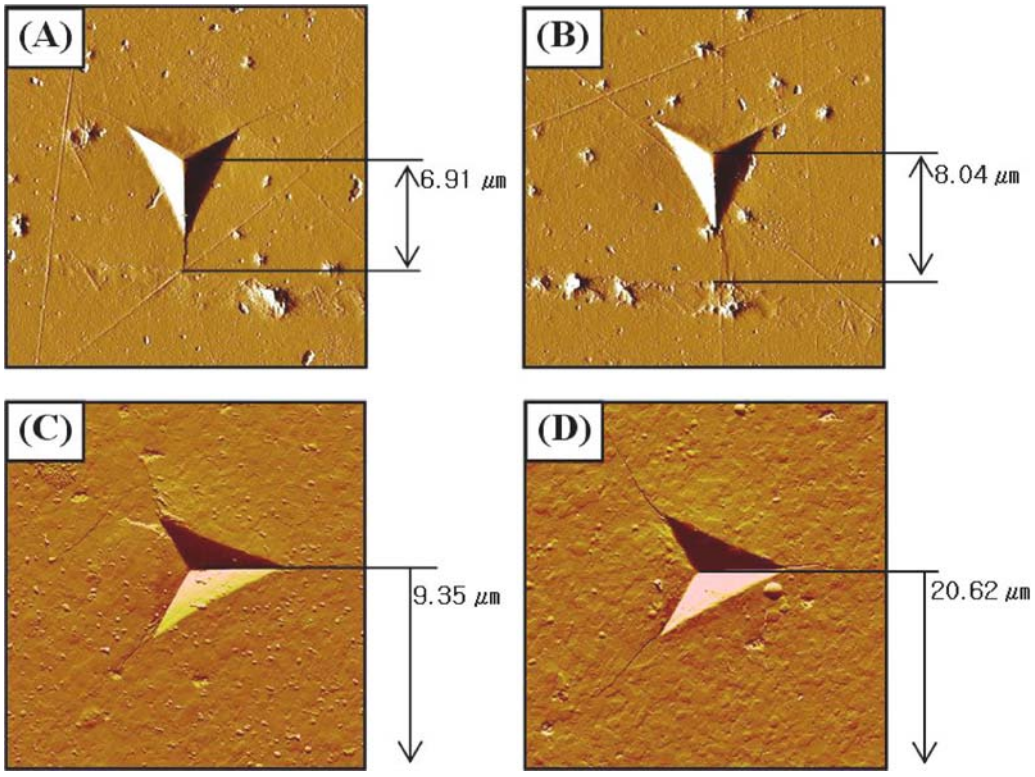

Fig. 2 AFM images of crack formation after indentation to 1250 nm: (A) standard MLCCs with external electrode in *x* plane, (B) same as (A) without external electrode, (C) post-heat treated MLCCs with external electrode in *y* plane, and (D) same as (C) without external electrode. The distance from internal electrode indicates beside each figure

Results and discussion

The *H* and *E* values measured by the nanoindentation are summarized at Table 1. The *H* and *E* values are not much affected by the plane, the external electrode, and the post-heat treatment, showing 11.5–12.0 GPa and 175–190 GPa, respectively. In the previous work [4], the *H* values obtained from Vickers indentation are 10.4 ± 0.5 GPa in the bulk samples and 9.3 ± 1.3 GPa in MLCCs. The *H* variation is related to the shrinkage difference between the inner parts and margins with and without the electrode, respectively, and to the microstructural defects [8, 9]. Therefore, it can assume that the different values between two indentation methods are due to the indenter size, because same MLCCs are employed for measurement and constrain effect of the external electrode can not be considered in the case without the external electrode in Table 1. However, the nanoindentation is a commonly used method to determine the mechanical properties of both bulk materials and thin films [10, 11].

Figure 2 shows the crack formation in the *x* and *y* planes for each case after indentation to 1250 nm. The cracks are well-developed at each corner. The crack length with the distance from the internal electrode was measured from AFM images in each plane, as functions of the external electrode and the post-heat treatment. Figure 3 shows the crack length measured at each penetration depth. The crack length in the *y* plane is longer than that in the *x* plane, indicating that relative smaller residual stress is created in the *y* plane. The

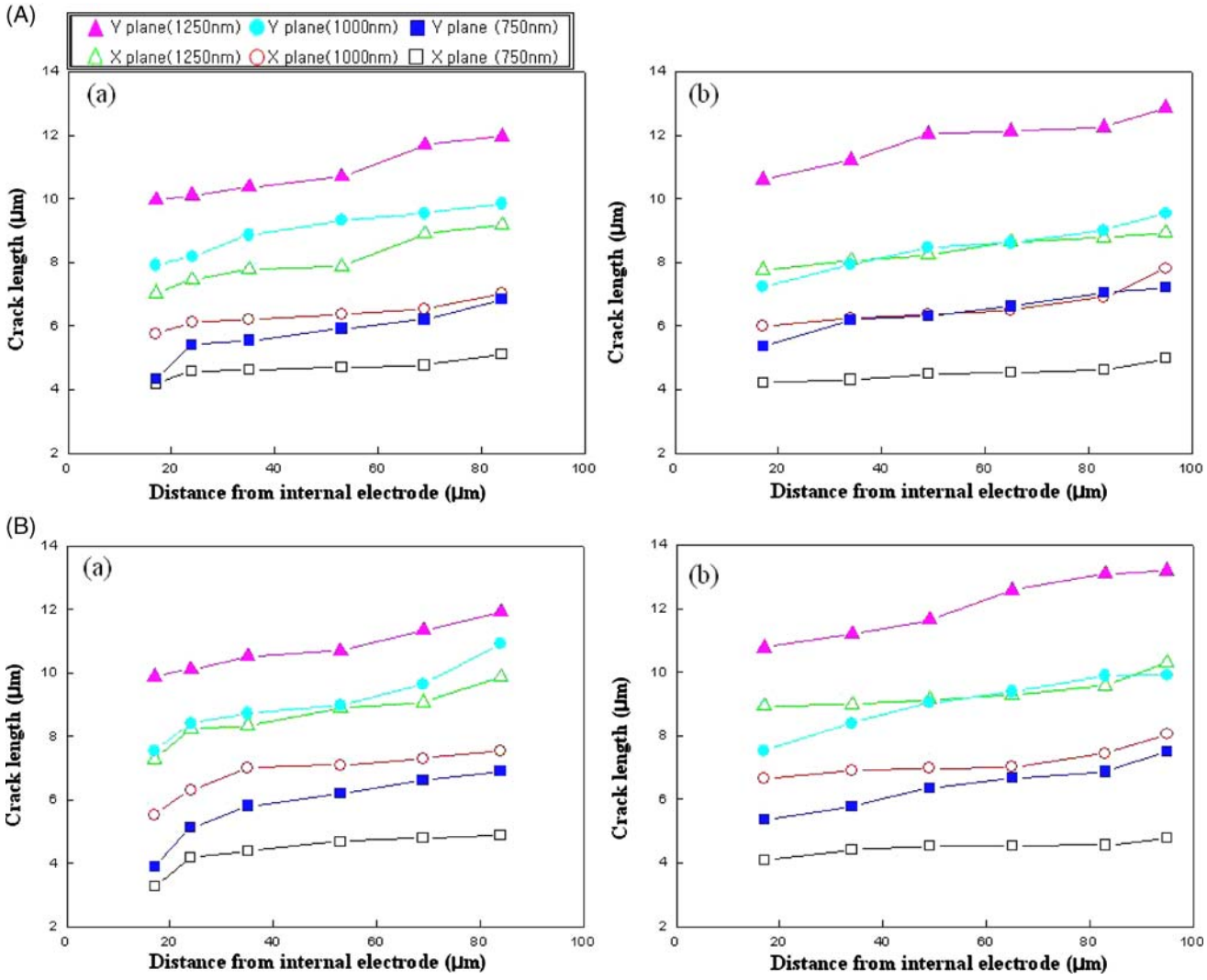

Fig. 3 Crack length versus distance from internal electrode in *x* and *y* planes of MLCCs as a function of penetration depth: (A) before and (B) after post-heat treatment. (a) and (b) indicate regions with and without external electrode, respectively

residual stress status of MLCCs without the external electrode is dependent on the direction—parallel and perpendicular to the internal electrode—in each plane, showing compressive and tensile residual stresses, respectively [12]. Meanwhile the compressive residual stresses are generated in all planes of MLCCs with the external electrode and the stress status is independent of the position, just showing higher residual compressive stresses at the direction perpendicular to the internal electrode, even though Vickers indentation method has been used to evaluate the stress status [13]. Therefore, the residual stress formed in each plane is compressive. The crack length is not affected by the post-heat treatment, which is gradually increased as the indentation position is far away from the internal electrode. The external electrode affects the crack formation in regions near to the internal electrode till 20 μm from the internal electrode, especially in the *x* plane.

The fracture toughness (K_{IC}) of the MLCCs depending on the external electrode and the post-heat treatment is shown in Fig. 4, in which "ST" and "900°C" indicate cases of without and with the post-heat treatment, and "with" and "without" mean cases of with and without the external electrode. The K_{IC} values in the *x* plane are larger than those in the *y* plane, independent of the external electrode and the post-heat treatment. In the *x* plane, the K_{IC} values in the regions with and without the external electrode show 1.32 $\pm$ 0.39 MPa·m$^{1/2}$ and 1.75 $\pm$ 0.29 MPa·m$^{1/2}$, respectively, without effect of the post-heat treatment. In the *y* plane, the K_{IC} values are not affected by the external electrode, showing 0.56 $\pm$ 0.10 MPa·m$^{1/2}$, even though the K_{IC} values are slightly increased to 0.73 $\pm$ 0.25 MPa·m$^{1/2}$ with the post-heat treatment. The K_{IC} values are well consistent with the crack formation, showing longer crack length in the *y* plane, because the residual stresses created on the MLCCs affect

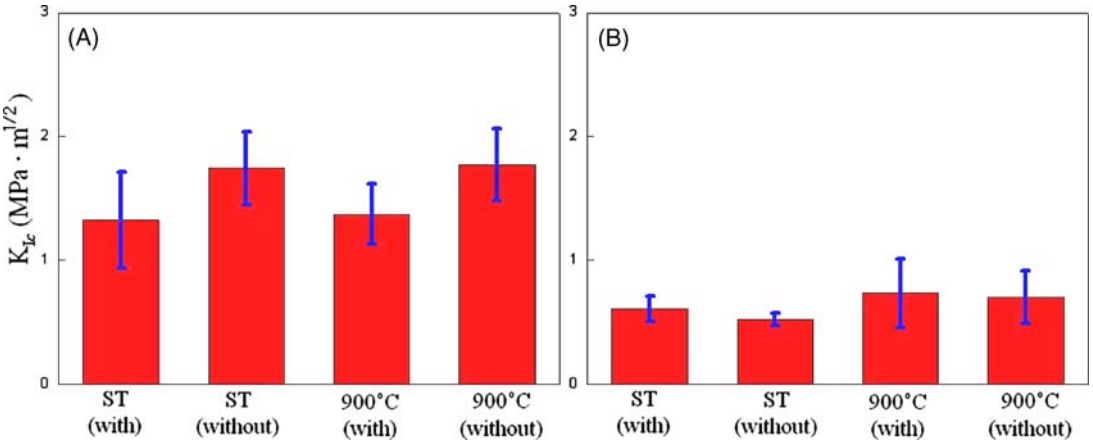

Fig. 4 Fracture toughness of MLCCs depending on position and post-heat treatment: (A) *x* plane and (B) *y* plane

the crack formation and propagation rather than mechanical properties. Consequently, it is found that the K_{IC} values in the *x* and *y* planes are affected by the external electrode and the post-heat treatment, respectively, even though the effect in the *y* plane is minor. The K_{IC} value obtained from Vickers indentation in the previous work shows the range of 0.75–0.90 MPa·m$^{1/2}$ in the bulk specimen, depending on the direction with respect to the lamination [4]. From which, it can be verified that the residual stresses formed during the fabrication process increase fracture toughness in the *x* plane and decrease in the *y* plane, which could not be released with the simple post-heat treatment.

Conclusions

The mechanical properties, *H* and *E*, of MLCCs are not much affected by the external electrode and the post-heat treatment, showing 11.5–12.0 GPa and 175–190 GPa, respectively. The crack length in the *x* plane is smaller than that in the *y* plane, which is gradually increased as the indentation position is far away from the internal electrode. The post-heat treatment does not affect the crack formation, whereas the external electrode affects, especially in the *x* plane, in regions near to the internal electrode till 20 μm. The fracture toughness, K_{IC}, in the *x* plane shows 1.32 ± 0.39 MPa·m$^{1/2}$ and 1.75 ± 0.29 MPa·m$^{1/2}$ for the MLCCs with and without the external electrode, respectively, without effect of the post-heat treatment. The K_{IC} values in the *y* plane are not much changed with the external electrode, showing 0.56 ± 0.10 MPa·m$^{1/2}$, even though the K_{IC} values are slightly increased to 0.73 ± 0.25 MPa·m$^{1/2}$ with the post-heat treatment.

Acknowledgment This work was supported by the Korea Institute S & T Evaluation and Planning (KISTEP) through the National Research Laboratory (NRL) and the Korea Research Foundation Grant (KRF-2004–005-D00111).

References

1. H. Cai, Z. Gui, and L. Li, *Master. Sci. Eng. B*, **83**, 137 (2001).
2. Y. Park, Y.H. Kim, and H.G. Kim, *Mater. Lett.*, **28**, 101 (1996).
3. S.-F. Wang and G.O. Dayton, *J. Am. Ceram. Soc.*, **82**, 2677 (1999).
4. D.H. Park, Y.G. Jung, and U. Paik, *J. Mater. Sci.*, **15**, 253 (2004).
5. C.R. Koripella, *IEEE Trans. Comp. Hybrids Manufact. Technol.*, **14**, 718 (1991).
6. W.C. Oliver and G.M. Pharr, *J Mater. Res.*, **7**, 1564 (1992).
7. M.T. Laugier, *J. Mster. Sci. Letters*, **6**, 355 (1987).
8. L. Karlsson, L. Hultman, and J.E. Sundgren, *Thin Solid Films*, **371**, 167 (2000).
9. J. Almer, M. Odén, and G. Håkansson, *Thin Solid Films*, **385**, 190 (2001).
10. M.F. Doerner and W.D. Nix, *J. Mater. Res.*, **1**, 601 (1986).
11. G.M. Pharr, *Mater. Sci. Eng. A*, **253**, 151 (1998).
12. S.G. Lee, U. Paik, Y.I. Shin, J.W. Kim, and Y.G. Jung, *Mater. Design*, **24**, 169 (2003).
13. D.H. Park, Y.G. Jung, U. Paik, J.W. Kim, and J.Y. Yu, *Mater. Sci. Forum*, **449–452**, 973 (2004).